

## Development of a Graphene Field Effect Transistor for GHz/THz Sensing

Alec Nicol  
Department of Chemistry  
University of Minnesota-Twin Cities  
Minneapolis, MN 55455

Graduate School of Advanced Integration Science  
Chiba University  
Chiba, Japan 263-8522<sup>1</sup>

Faculty Advisor: Dr. Yuichi Ochiai<sup>1</sup>

### Abstract

A small bandgap matched to low energy photons and a Dirac electron transport system are two definitive characteristics of bilayer graphene (BGR) that has gained it considerable interest in realizing a broadly tunable sensor for application in the microwave (GHz) to terahertz (THz) regimes. For these reasons, graphene field effect transistors (GR-FETs) have the potential to exceed the detection limit of most existing semiconductor quantum point contacts (QPCs). This is due to the unique phase coherent length of open quantum-dot structures formed in bilayer graphene when exposed to GHz/THz radiation. Existing GR-FETs have been fabricated by micromechanical exfoliation of highly oriented pyrolytic graphite (HOPG-SG2) contacted with submicron-scale metal electrodes (Ti/Au or Pd/Au). The microwave transconductance characteristics show excellent photoresponse around the X band (~10 GHz) and are predicted to have continued sensitivity in the THz range after the measurement setup is optimized. Herein, improvements to the wiring setup, sample box architecture, graphite source, and bolometric heating of the GR-FET sensor were made in order to extend microwave photoresponse to 40 GHz and further improve THz detection. Future studies will include THz irradiation experiments (300-3000 GHz) using the same optimized experimental setup. THz photoresponse in this range will be important for future developments in medical imaging, spectroscopy, and communication which all exploit the unique linear non-ionizing benefits of THz radiation.

**Keywords:** Graphene, Field Effect Transistor (FET), Terahertz (THz)

### 1. Background

Graphene (GR) is a two-dimensional network of  $sp^2$  hybridized carbon atoms packed into a hexagonal lattice and is the basic building block for higher order graphitic materials.<sup>1</sup> Graphene has become one of the most well-known carbon nanomaterials due to its unique optical, electrical, and thermal properties.<sup>2</sup> The unique band structure of graphene is governed by a quasi-Dirac electron system that varies from the single layer case with gapless spectrum characteristics to the bilayer case with a small bandgap.<sup>1</sup> In both instances, the bandgap can be broadly tuned in order to match low (meV) energy photons in the GHz/THz regime, in marked contrast to conventional semiconductors whose bandgaps appear several orders of magnitude larger.<sup>3</sup> The observation of quantum fluctuations in the magnetoresistance of open quantum dot structures in graphene indicates the presence of discrete quantized states, which are thought to be particularly useful in GHz/THz sensing. For these reasons, graphene field effect transistors (GR-FETs) have the potential to exceed the detection limit of most existing semiconductor

quantum point contacts (QPCs).<sup>4,5,6</sup> Additional benefits to the GR-FET platform relative to structures based on carbon nanotubes include a high level of similarity with conventional integrated semiconductor FET fabrication techniques. Considering the mentioned benefits, GR-FETs are emerging as excellent candidates for developing a broadly tunable GHz/THz sensor. In particular, the realization of THz detection will be important for future developments in medical imaging, spectroscopy, and communication which all exploit the unique linear non-ionizing benefits of THz radiation.<sup>7</sup>

Existing GR-FETs have been fabricated by micromechanical exfoliation of highly oriented pyrolytic graphite (HOPG-SG2) contacted with 2-terminal submicron-scale metal electrodes (Ti/Au or Pd/Au).<sup>8</sup> The microwave transconductance characteristics show excellent photoresponse around the X band (approximately 10 GHz) but quickly cuts-off thereafter. The observed cut-off frequency was determined to be a result of the measurement wiring rather than the intrinsic response of the graphene. The positive results of this study indicate that THz detection is likely and that many of the same experimental setup components could remain constant if THz irradiation experiments were preformed. Therefore, improvements to the wiring setup, insulation architecture, graphite source, and heat dissipation of the GR-FET sensor were made in order to extend microwave photoresponse to 40 GHz and further improve THz detection.

## 2. Methods

The devices used in this experiment were fabricated following an established procedure.<sup>8</sup> Thin graphite flakes were exfoliated from natural Kish graphite using adhesive tape and transferred onto a conducting p-type Si substrate with a 300-nm-thick SiO<sub>2</sub>. Thermal annealing (400°C, flow rate of 4.3 L/min using Ar/H<sub>2</sub>, 5 min) was necessary to remove residual tape adhesive and ambient molecules from the Si substrate surface. The thin graphite flakes were imaged under an optical microscope as seen in Figure 1c and 1d. Single and bilayer flakes were identified by examining the light intensity shift in the green channel of the blue-green-red scale relative to the contiguous substrate. Photolithography was used to form a submicron scale two-terminal Ti/Au (50/100 nm thick, respectively) contact design with a gap of 10 μm as seen in Figure 1a. Overall, one single layer and one bilayer GR device were fabricated for this study. Figure 1c shows the bilayer flake with an area of 300 μm<sup>2</sup> and an atomic thickness of 6-8 Å. Figure 1d shows the monolayer graphene flake with an observed area of 200 μm<sup>2</sup> and an approximate atomic thickness of <6 Å. These sizes are comparable to previous experiments so a quasi-ballistic or weakly diffusive transport mechanism is expected.<sup>3</sup> Back-gate dependence measurements were conducted at room temperature by varying the DC two-terminal current as a function of the gate voltage. The Dirac point or minimum conductivity point was located around 35 V for both samples as seen in Figure 4b.

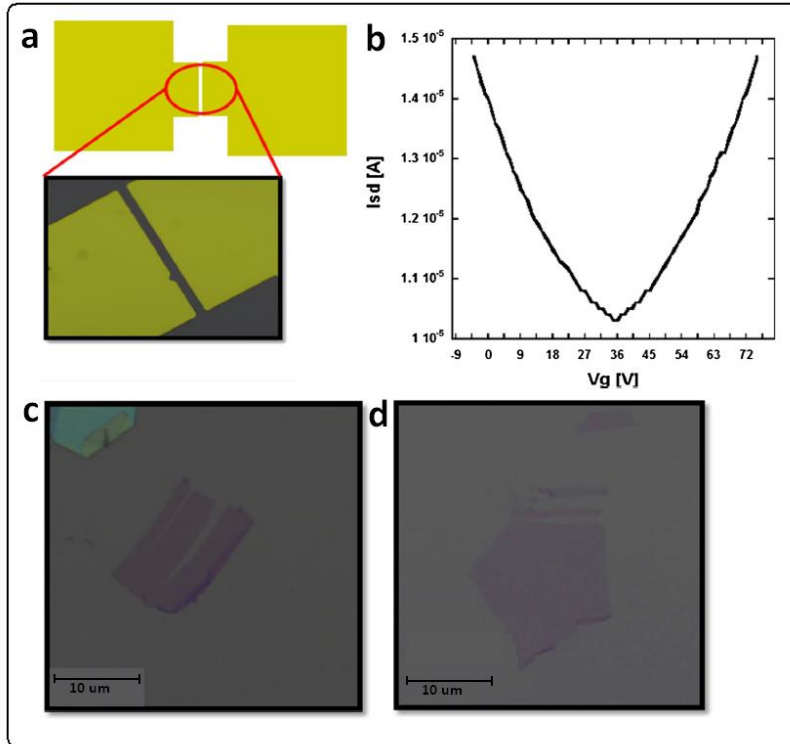


Figure 1. GR-FET Detector Characteristics (a) Basic two-terminal metal contact system. (b) Gate voltage dependence at room temperature with observable Dirac point. (c) Bilayer GR, area of  $300 \mu\text{m}^2$  and atomic thickness of 6-8 Å. (d) monolayer GR, area of  $200 \mu\text{m}^2$  and atomic thickness of  $<6 \text{ \AA}$ .

GHz frequency response measurements were taken at room temperature up to 40 GHz at zero back-gate voltage using an improved experimental setup as seen in Figure 2a. The actual sample box is shown in Figure 2b. Structural changes are highlighted in the discussion later on. The GR-FET was mounted on a Cu platform connected to a current source where a back-gate voltage could be applied. Direct Au/Cu-lead wire connections allowed a 40 GHz signal (Anritsu MG3694B) to be sent directly through the device to a power sensor (Tektronix CSA8200). Subminiaturetype K (SMK) connectors with cut-off frequencies at 40 GHz provided a means to connect ATEM cables to the Cu wires.

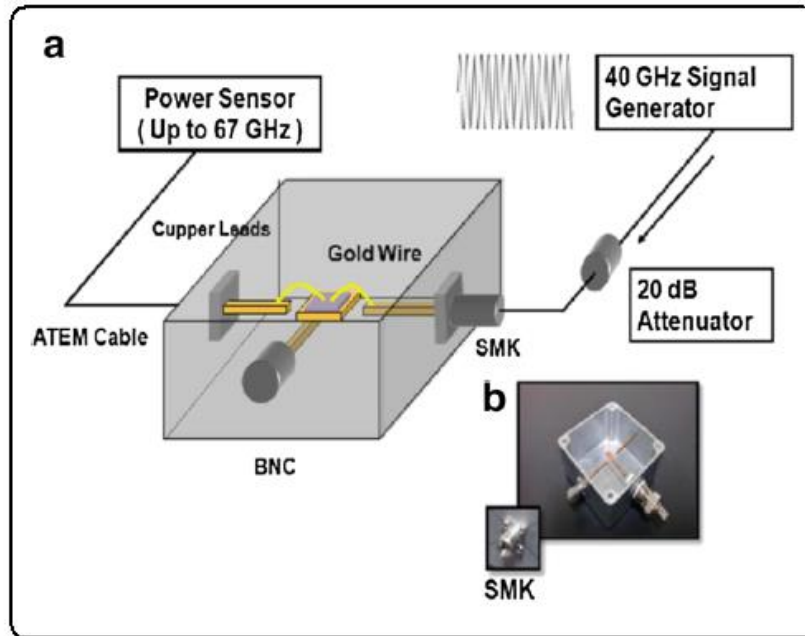


Figure 2. GHz Frequency Response Experimental Setup (a) Modified box with floating lead connections that have drastically reduced the surface resonance effects and parasitic capacitance. (b) Actual sample box.

### 3. Results and Discussion

GHz frequency response was recorded up to 40 GHz for both the single and bilayer GR-FET at zero gate voltage as seen in Figures 3a and 3b, respectively. The composite response of the device/wiring is shown in blue whereas the green-dottedplot shows the response of just the wiring (Au/Cu directly connected to the back gate platform as seen in Figure 2a). The wiring has a low GHz frequency response from microwave resonances arising from commensurate conditions between the microwave signal and the characteristic length of the circuit, mainly the metal plate stage and the Cu lead contacts.<sup>9,10</sup> The single layer GR-FET does not meet a cutoff frequency as previously reported<sup>8</sup> and extends to at least 40 GHz whereas the bilayer GR-FET starts to diminish around 30V. In the single layer case, an absence of a bandgap results in a higher charge carrier mobility which increases the overall microwave transconductance capabilities of the device. Although resonance frequency noise exists from the device itself, the microwave response is strong enough to dominate the signal. This is not the case for the bilayer device where the resonance frequency can be seen to dominate the signal because of a relatively low charge mobility due to the presence of a bandgap. Regardless, the frequency response was extended at least 15 GHz from previous reports.<sup>8</sup>

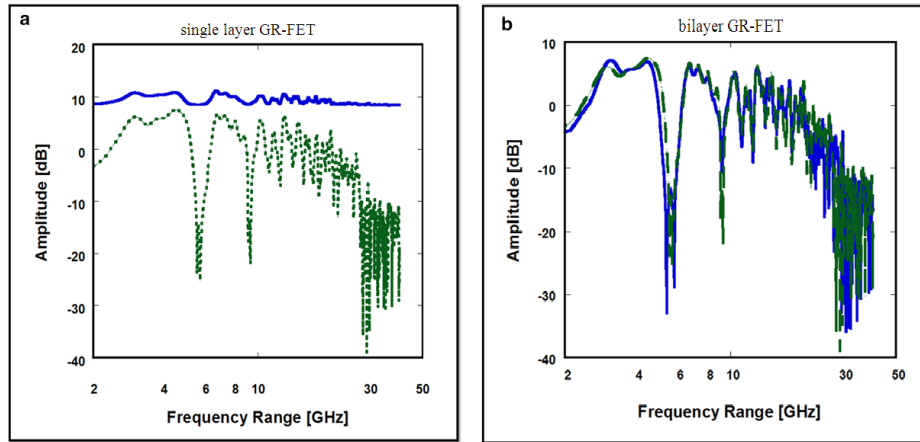


Figure 3. GHz Frequency Response Profile up to 40 GHz (a) Single layer GR-FET (b) Bilayer GR-FET.

The gains in GR-FET response can be attributed to the improved experimental components as shown in Figure 2a. Modifications, such as suspending the device using Cu/Au wires rather than having it rest on an insulating substrate were found to greatly reduce parasitic capacitance and increase the detection limit of the device. As discussed previously, using subminiature type A (SMA) connectors presented a major limitation in the previous setup and affected the total response cutoff. Additionally, possible parasitic capacitance was drastically reduced using this setup because our device was not resting on an insulating coplanar waveguide (CPW) as previously reported.<sup>8</sup> Although CPWs provide a surface-strip transmission line, the direct dependence of the characteristic impedance on the thickness of the dielectric substrate and its poor heat dissipation presented an increasingly complex set of challenges for GHz/THz sensing.<sup>11</sup> In particular, poor heat dissipation becomes a problem at higher THz frequencies where the influence of bolometric and nonlinear effects dominate the device response. The improved experimental setup has high heat dissipation and can easily be modified to incorporate a heat sink so that thermal noise is minimized. In our recent attempt, SMK connectors and cables were used which have a higher cutoff frequency at 40 GHz. Therefore, the device response was predominantly limited by surface wave resonance effects from the metal plate stage and the lead contacts as demonstrated in Figure 2a. The device response shows possible conduction modes for the GR device up to 40 GHz, indicating that the ‘yield’ has drastically increased. At higher frequency regimes, a greater gain in amplitude relative to the starting point is observed, showing that the transport modes dominate the device performance as shown in Figures 3a and 3b.

#### 4. Conclusion

In summary, the microwave frequency response of both a single and bilayer GR-FET was significantly extended from previous reports by improving the wiring setup, insulation architecture, and heat dissipation of the GR-FET sensor. A single layer GR-FET showed extended response to at least 40 GHz whereas the bilayer GR-FET encountered a cutoff frequency around 30 GHz. The superior GHz frequency response for the single layer GR-FET can be attributed to high charge mobility which remarkably persists even at room temperature. Therefore, it is reasonable to conclude that this improved GR-FET detector system serves as a functional means to analyze high-frequency GHz response measurements. Future studies will include applying this improved detection system to THz frequency response experiments and testing variable back gate voltages.

#### 5. Acknowledgements

This work is supported in part by Grants-in-Aid for Scientific Research from the Japan Society for the Promotion of Science (19054016, 19204030, and 16656007) and by the JSPS Core-to-Core Program. This work was also in part supported by the Global COE Program at Chiba University (G-03, MEXT) and promoted by the international research and educational collaboration between Chiba University and SUNY Buffalo. Acknowledgement is extended

to the National Science Foundation's Partnerships for the International Research & Education (NSF-PIRE) grant (OISE-0968405).

## 6. References

1. Novoselov, K. S. *et al.* Two-dimensional gas of massless Dirac fermions in graphene. *Nature* **438**, 197–200 (2005).
2. Geim, A. K. & Novoselov, K. S. The rise of graphene. *Nature Materials* **6**, 183 (2007).
3. Ujiie, Y. *et al.* Regular conductance fluctuations indicative of quasi-ballistic transport in bilayer graphene. *Journal of Physics: Condensed Matter* **21**, 382202 (2009).
4. Song, J. W. *et al.* Terahertz response of quantum point contacts. *Applied Physics Letters* **92**, 223115–223115–3 (2008).
5. Song, J. *et al.* Evaluating the performance of quantum point contacts as nanoscale terahertz sensors. *Opt. Express* **18**, 4609–4614 (2010).
6. Russo, S. *et al.* Observation of Aharonov-Bohm conductance oscillations in a graphene ring. *Physical Review B* **77**, (2008).
7. Nguyen, T. K., Han, H. & Park, I. Full-Wavelength Dipole Antenna on a Hybrid GaAs Membrane and Si Lens for a Terahertz Photomixer. *J Infrared Milli Terahz Waves* **33**, 333–347 (2012).
8. Mahjoub, A. M. *et al.* Towards Graphene GHz/THz Nanosensor. *Jpn. J. Appl. Phys.* **50**, 070119 (2011).
9. Gay, J. G., Smith, J. R. & Arlinghaus, F. J. Large Surface-State/Surface-Resonance Density on Copper (100). *Phys. Rev. Lett.* **42**, 332–335 (1979).
10. Billington, R. L. & Rhodin, T. N. Surface Resonance on W(100): Effects of Au and Cu Adsorption. *Phys. Rev. Lett.* **41**, 1602–1605 (1978).
11. Wen, C. P. Coplanar Waveguide: A Surface Strip Transmission Line Suitable for Nonreciprocal Gyromagnetic Device Applications. *IEEE Transactions on Microwave Theory and Techniques* **17**, 1087 – 1090 (1969).